Indoor Propagation Characteristics at 5.2GHz in Home and Office Environments

Hyun Kyu Chung and Henry L. Bertoni

Abstract: **This paper presents results of continuous wave and swept frequency response measurements over the frequency range of U-NII lower and middle bands from 5.15GHz to 5.35GHz in indoor environments. From the continuous wave measurements at 5.2GHz, the excess path loss, and the statistical characteristics of the temporal and spatial fading were found. By sweeping the frequency over the band, envelope correlation as a function of frequency was found and the coherence bandwidth (CBW) was determined from the envelope correlation. Using a channel model, the CBW was used to evaluate RMS delay spread. The dependence of CBW on the antenna polarization was simulated and compared with the measurement results. The influence of room size and separation of transmitter and receiver for LOS paths on RMS delay spread was discussed.**

Index Terms: **Indoor propagation, narrowband measurement, wideband measurement, rms delay spread, coherence bandwidth.**

I. INTRODUCTION

The FCC released a new frequency band of 300MHz width just above 5GHz that has been called the Unlicensed National Information Infrastructure (U-NII) band to provide for mobile multimedia applications. Thereafter IEEE 802.11 in U.S., ETSI BRAN(Broadband Radio Access Network) in Europe, and MMAC(Multimedia Mobile Access Communication) in Japan, selected OFDM as the basis of their physical layer technology for data rates from 6 up to 54 Mbps in this band[1], [2]. The deployment of low power wireless systems in the 5GHz band for home office and related applications will require a knowledge of the path loss for distances up to 10's of meters within and around the buildings. The design of systems using OFDM technology also requires knowledge of the channel parameters such as the coherence bandwidth and delay spread. The coherence bandwidth is of importance in estimating the simultaneous fading of adjacent tones, while the delay spread is needed to set the guard time. Recently, extensive measurements in this band were made and reported [3]–[10].

This paper describes the measurement of continuous wave (CW) propagation at 5.2GHz and swept frequency (SW) response over the frequency range from 5.15GHz to 5.35GHz in indoor environments of an office building and residential houses. The program of measurements is intended to evaluate the path loss, and coherence bandwidth in indoor environments. These measurements supplement recent measurement in the U-NII band of path loss and delay spread [3]–[10]. Over small areas, path loss will depend on the transmission loss through walls and floors, as well as the free space loss. In order to calibrate the measurement system, the antenna characteristics in an open area were measured and used as a reference for indoor links with blockages

In the CW measurements, received power (Prx) was measured at various locations with line-of-sight (LOS) and non-line-of-sight (nLOS) paths over the links that are up to 20m. For residential houses, the path loss was measured over links that go from inside the house to outside locations, and between floors. In nLOS paths, blocking objects between transmitter and receiver are mainly internal walls, external walls and floors. Analysis of the results includes the dependence of the small area average path loss on the distance between transmitter and receiver, excess path loss, and the statistical characteristics of the temporal and spatial fading, as well as polarization effects.

In the SW measurements, the transmitting system (Tx) steps through the frequencies in the range 5.15–5.35GHz, while the receiving system (Rx) gathers the power level at each frequency. Various locations having LOS and nLOS paths were tested for these measurements. For calibration purposes, the frequency dependence of the colinear antennas was first obtained for vertical and horizontal polarization in an open area. The measured data was refined through the procedure of adjustment and interpolation, which are used to compensate for the measurement system effects. Envelope correlation coefficients of the resulting channel response were analyzed to give a proper evaluation of the coherence bandwidth (CBW). Based on a realistic channel model, the CBW was used to evaluate the RMS delay spread. The measurement results also show that room size and distance between transmitter and receiver for LOS paths influence the RMS delay spread.

II. DESCRIPTION OF THE MEASUREMENTS

A. Measurement System

The measurement system is depicted in Fig. 1. The transmitter is an RF signal generator (SMT-06, Rohde & Schwartz) feeding a vertically polarized colinear antenna through a low loss coaxial cable (8301, Midisco). This antenna is fixed to a wooden mast, which is attached to a mobile plastic cart. The cable is 0.9m long and has a loss of 1.2dB at 5.2GHz. Two identical omni-directional colinear antennas were used for the

Manuscript received December 17, 2001; approved for publication by Yoshihide Yamada, Division II Editor, September 6, 2002.

H. K. Chung is with senior research staff in Electronics and Telecommunications Research Institute (ETRI), Korea.

H. L. Bertoni is with professor of Polytechnic Univ. in Brooklyn, New York, USA.

This work was funded by Sharp Laboratory of America.

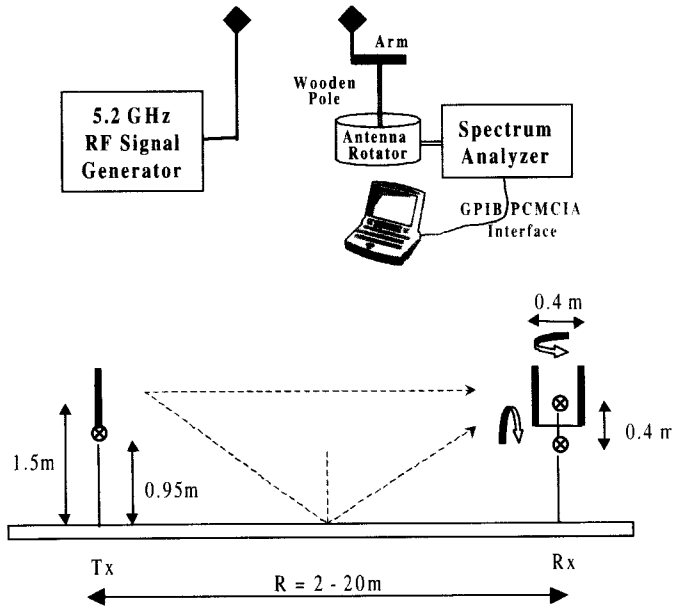

Fig. 1. Description of the measurement system for vertical and horizontal polarization.

transmitter and the receiver. The antenna consists of vertically stacked elements that provide a reported vertical beamwidth of 14° while maintaining a uniform omni pattern with 9dBi gain in azimuth.

The receiver consists of an identical colinear antenna feeding the spectrum analyzer (HP8561E) through 1.8m flexible coaxial cable with a loss of 2.6dB (RG142). The spectrum analyzer is remotely controlled by a laptop computer via a GPIB/PCMCIA interface. Using Labview software, the laptop computer collects the received power data in dBm from the spectrum analyzer for a given duration with a programmed sampling rate. The receiver system is also mounted on a mobile plastic cart for easy movement. The receiving antenna is secured to a wooden arm of length 70cm that is mounted on an antenna rotator, rotating at a constant speed of one revolution per 60seconds. The rotator itself is fixed to the top surface of the cart.

For vertical polarization measurements, the center of the transmitting and receiving antennas are at a height of 1.5m above the floor, which is enough to avoid blocking of the signal path by the mobile carts and other equipments. In making path loss measurements between floors, the horizontal polarization was used to avoid effects of the vertical antenna patterns. For the horizontal polarization measurements, the transmitting antenna was fixed parallel to the floor at a height of 95cm. The axis of the receiving antenna rotator in this case was oriented parallel to the floor at a height of 95cm.

B. Range Dependent Characteristics

The measurement system was calibrated at 5.2GHz in an open area at distances up to 20m. As in all path loss measurements, the receiving antenna was rotating around a circle, and the powers in watts measured at each point along the circle were averaged to obtain the small area average. Beyond the far field distance of the antenna, the measurements were fit to a path loss formula of the form

$$PL = A - 10u \log R, \tag{1}$$

where u is the path loss index and A is a constant. From the least squares fit, it was found that the path loss index is 2.08 and 1.95 for vertical and horizontal polarizations respectively, which agrees well with the free space path loss index for a point source. The received powers in dB of the least squares fit line for each polarization are given by

$$P_{ver} = -20.82 \log(R) - 27.56, \quad 2m \leq R \leq 20m, \tag{2}$$

$$P_{hor} = -19.52 \log(R) - 32.42, \quad 2m \leq R \leq 20m. \tag{3}$$

It is seen that this fitting result gives a good agreement with measurements for distances in the range from 1.8m to 21m. The excess path loss at a given receiver location is defined as the difference between the small area average power level and the reference level given by (2) or (3).

C. Frequency Dependent Characteristics

In order to remove the effect of the frequency dependence of the measurement system on the swept frequency response, the frequency response of the measurement system was found in an open area over the frequency range from 5.15GHz to 5.35GHz. The transmitter slowly steps the signal frequency over the foregoing range, while Rx measures the power level at each frequency at a fixed Rx position. The received power normalized to its average represents the free-space frequency response of the measurement system itself and is used to remove the measurement system effect from the measured data. For a fixed distance between Tx and the axis of the Rx antenna rotator, the SW measurements were made at either 16 or 24 equally spaced positions of Rx around the rotator circle. At each of these Rx positions, the frequency response was obtained. For more accuracy, the above procedure was repeated with different distances between two antennas and different polarizations in an open area. For vertical polarization, the frequency response measurements were repeated at distances of 4.6m, 9.1m, and 21m between Tx and Rx, which gave total 45 different data sets. For horizontal polarization, 24 different data sets were obtained at a distance of 9.1m.

All measured data sets were normalized to the LSE polynomial for each polarization. The fitting curves in dB are given by the polynomials,

$$Offset\_hor = 3.89 - 5.96 \times 10^{-3} * \Delta f - 4.97 \times 10^{-4} * (\Delta f)^2 + 1.66 \times 10^{-6} * (\Delta f)^3, \tag{4}$$

$$Offset\_ver = 4.80 + 1.28 \times 10^{-2} * \Delta f - 9.26 \times 10^{-4} * (\Delta f)^2 + 3.13 \times 10^{-6} * (\Delta f)^3. \tag{5}$$

where Δf = *frequency[MHz] − 5150.* These expressions are used to remove the measurement system effect from the measured frequency response at indoor locations.

D. Measurement Procedure

The CW measurements consist of two parts, one made while the receiver rotates continuously around a circle of about 22λ circumference during 60 seconds, and the other temporal measurement at a fixed receiver position. During the continuous rotation of the receiving antenna around a circle, 600 readings of the received power were collected over 60 seconds from the spectrum analyzer. The mean value of the 600 received power readings represents the small area average received power at that location [11], [12]. For the second measurement, the receiver was located at a position on the circle where the time average is approximately equal to the spatial average. While the receiver is stationary at this position, 600 data readings are collected over a 60 second interval. The rapid variation of the received power as a function of time gives the temporal fading characteristic, and the average values over time as a function of the receiver position gives the spatial fading characteristic. Throughout measurement procedure, the transmitter power was kept at 10dBm and all cable connections were kept unchanged. When making measurements with Tx and Rx in different rooms on different floors, Tx and Rx are not only horizontally polarized, but also aligned so that the broadside directions are aimed at each other.

For the SW frequency measurements, the indoor environment is assumed to be a time invariant channel. Measurements were carried out avoiding possible movements inside the buildings. The transmitter was set to step through the frequency range from 5.14GHz to 5.36GHz . The step size is 1MHz and the dwell time is 500 msec for each frequency step. A sweeping period of 110 sec is needed to cover the total span of 220MHz. The spectrum analyzer is set to have a 220MHz span centered at 5.25GHz with 300KHz resolution bandwidth, which provides 50msec sweep time. In order to get stable data acquisitions, Labview was programmed to read and store the received power every 100msec which is twice of the sweep time of the spectrum analyzer. At every 100msec the peak power value in dBm, and its corresponding frequency, are recorded from the spectrum analyzer to the laptop computer. Since Tx transmits CW signals for 500msec at a given frequency, 5 data readings at Rx are possible for each frequency step. If the channel is time invariant and the measurement system is ideal, the 5 frequency responses for each frequency will have the same value.

III. SITE ENVIRONMENT FOR INDOOR MEASUREMENTS

CW and SW measurements were carried out in five different buildings. The first (Office 1) is an office building of modern construction with gypsum board interior walls and concrete over metal pan floors. The other buildings are wooden-frame, two story single-family houses (House 1–3) in New Jersey and a wooden-frame, three story single-family row house (House 4) in Brooklyn, New York.

The layout of a 32 m x 23 m portion of the basement floor of Office1 is shown in Fig. 2. It consists of several engineering laboratories surrounded by rooms of different sizes. All of the rooms in Fig. 2 are surrounded by a hallway. The internal walls of this building are made of gypsum board on metal studs. Room A and H are research labs divided by movable partitions, which are 1.6 m high and made of wood and fabric with metal frames. Rooms B, C, D, I, and F are engineering laboratories, which contain metal cabinets and metal frame workbenches with wooden tops and metal shelves for lab activities. The 1.8m wide and 1.2m high workbenches are connected along the walls. In the storage rooms, 1.8m high metal cabinets are connected along the walls on both sides of the rooms. The other rooms are used for private offices and computer labs with standard office furniture. The nonmetallic acoustic ceiling tiles are supported by metal grids, 3m above the floor which is made of concrete. The doors are made of metal and are usually closed, and there are no windows in any rooms. For the CW measurements, the transmitter was located at the center of room O. In room O, receiver locations include LOS paths indicated 'O' and partially obscured paths indicated by '•'. The blockage is due to workbenches and metal cabinets located in the center of room O. The other uppercase block letters in Fig. 2 indicate various receiver locations in the different rooms. For SW measurements, Tx was located in room C. For a fixed distance between Tx and the axis of the Rx antenna rotator, the SW measurements were made at 16 equally spaced positions of Rx around the rotator circle.

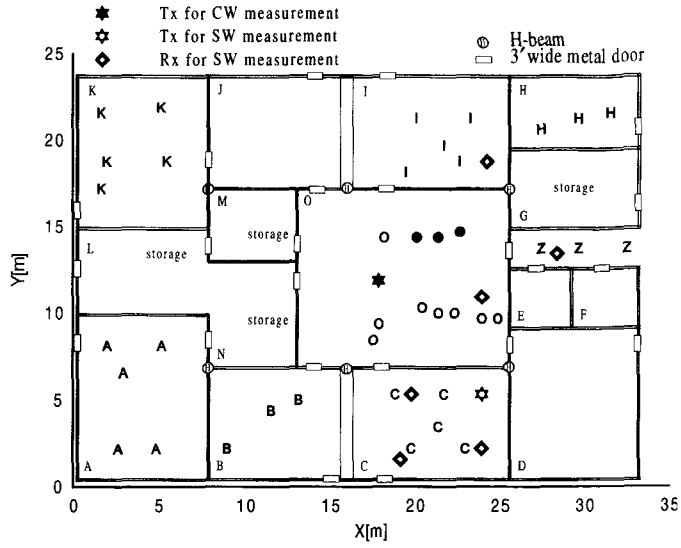

Fig. 2. Floor plan of Office1 with transmitter and receiver locations for CW and SW measurements.

House 1 is a 20 year old suburban house constructed in the raised ranch style and sits on a lot of dimensions 15m x 38m. The house has carpeted hardwood floors, with internal walls made of gypsum board on wood studs separated by 41cm. The inner wall is about 12.7cm thick and the exterior wall is about 20cm thick with a insulation material inside. The height of ceiling is 2.4 m on the 2^{nd} floor and 2.3m on the 1^{st} floor. The thickness of the floor and ceiling between the 1^{st} floor and the 2^{nd} floor is 28cm. The house has steam heating and separate air conditioning for each room. Fig. 3(a) shows the 2^{nd} floor layout of the house. The transmitter was placed in a corner of the living room, and the receiver placed on LOS paths in the living room and nLOS paths in other rooms. It is noted that one of the locations 'C' in the kitchen and one of the locations 'Z' in the hallway are partially obscured. Except for the metal refrigerator located at the lower left corner in the kitchen, standard

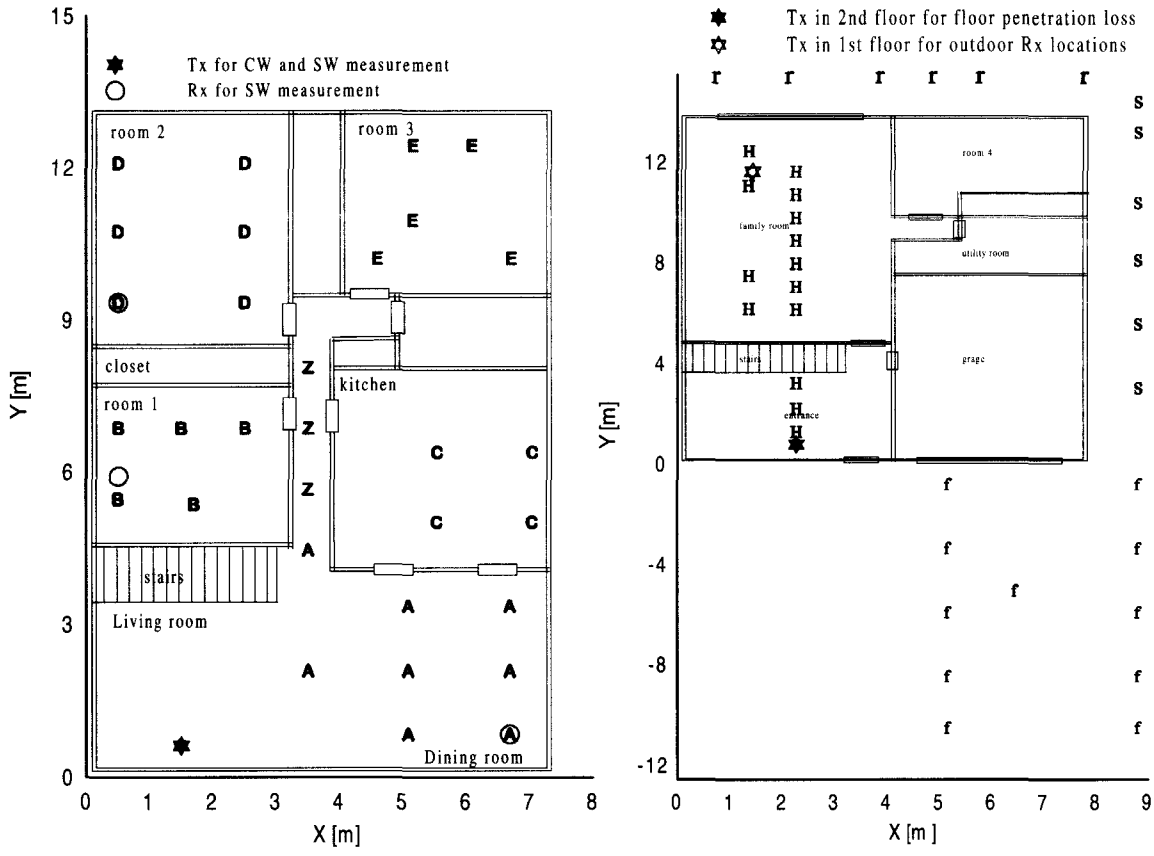

(a) the second floor.

(b) The ground level with the first floor.

Fig. 3. Floor plan of House1 with transmitter and receiver locations for CW and SW measurements .

home furniture in all rooms are made of wood. For a fixed distance between Tx and the axis of the Rx antenna rotator, the SW measurements were made at 16 equally spaced positions of Rx around the rotator circle. Fig. 3(b) shows the ground level of the house with the transmitter and receiver locations in and around the house. For the path loss measurement between floors, the horizontally polarized transmitter was placed on the 2^{nd} floor and the receiver at locations 'H' on the 1^{st} floor, with the beams of the antennas aimed at each other. For the outdoor measurement, the antennas were oriented vertically with the transmitter placed inside the house (in the corner of family room), and the receiver at location at the front ('f'), side ('s'), and rear ('r') of the house.

House 2 is a 20 year old suburban, two story house, with the rooms at the back of the house raised one half story so that there are four different floor levels. The flooring is hardwood with partial carpeting. It sits on a lot of dimensions 24m x 30m. The four floor levels consist of the basement level, family room level, living room level and bedroom level. Starting at the basement, the four different levels are overlapped in height by 1.17m, 1.24m, and 1.45m in sequence. The heights of ceiling are 2.1m basement, 2.4m family room level and 2.5m living and bedroom. The internal walls have thickness of 12cm, and are made of gypsum board on wood studs separated by 41cm. The exterior wall is about 20 cm thick with insulation materials inside and covered by plywood and metallic sidings. The thickness between the floor and ceiling is 28cm. House 2 has a centralized heating and air conditioning systems with air supplied through metallic ducts located in the floors. Even though House 2 has many windows, there is significant radio attenuation from inside to outside due to the metallic siding. Fig. 4(a) shows the floor layout and antenna placements for CW measurements in House 2. The living room and kitchen are on the same level and the basement is underneath them. The Rx locations 'L' and 'K' are on the same level as Tx. However, 'B', 'O', and 'F' are on a lower level than Tx, while '1' and '2' are on a higher level than Tx. Horizontal polarized measurements were carried out at all locations indicated in Fig. 4, and vertical polarized measurements were repeated at the same locations in the kitchen and the living room. For all measurements, Tx was placed in a corner of the living room as indicated by the star. The receiver was placed on LOS paths in the living room and nLOS paths in other rooms. Each Rx location is indicated by the first letter of its corresponding room. Except for the metallic refrigerator located against a wall in the kitchen, the furniture in all rooms was standard and made of wood. For a fixed distance between Tx and the axis of the Rx antenna rotator shown in Fig. 4(b), the SW measurements were made at 24 equally spaced positions of Rx around the rotator circle.

House 3 is a wooden-frame, two story single-family structure that is six years old. It has a full basement and gypsum board interior walls. The first and second floors are of hardwood and

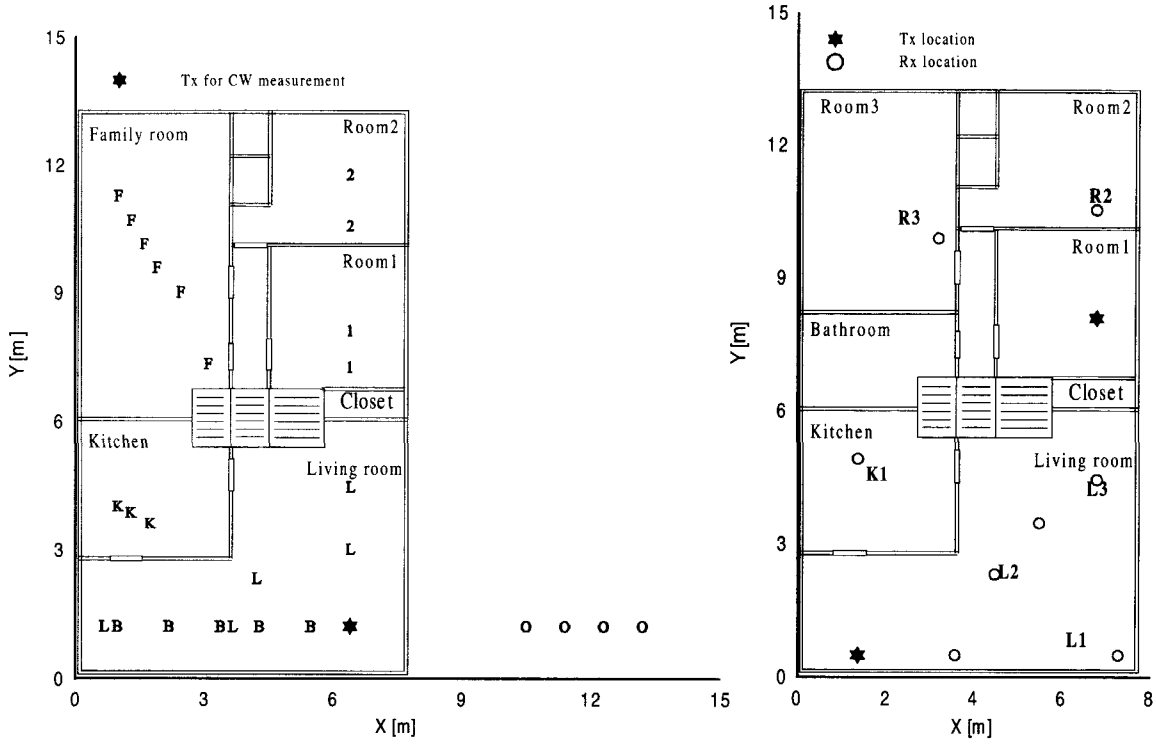

(a) CW measurements. (b) SW measurements.

Fig. 4. Floor plan of House2 with transmitter and receiver locations for CW and SW measurements.

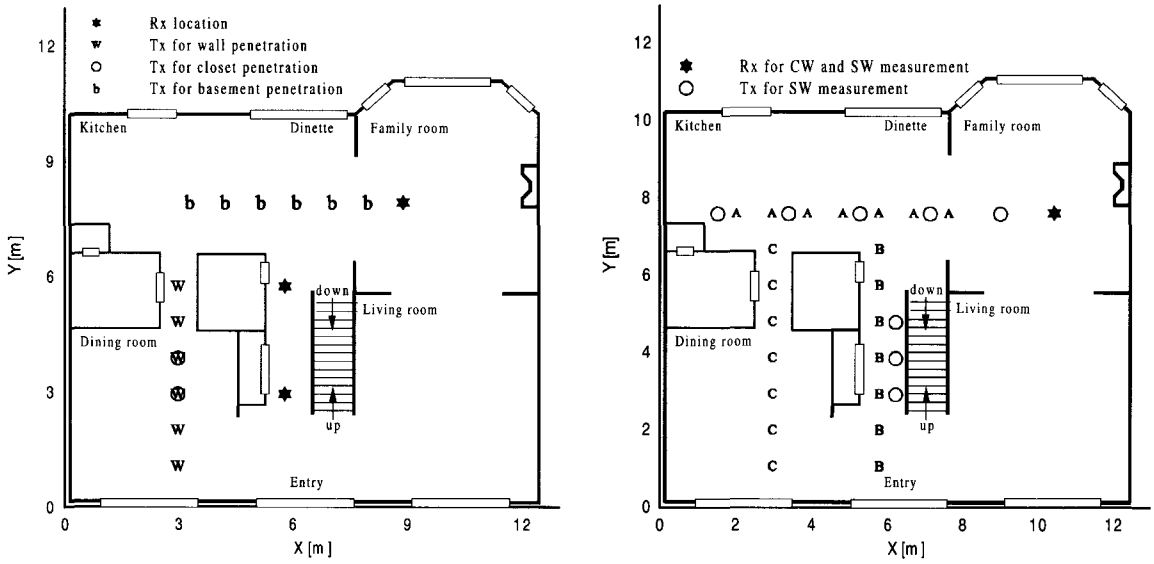

a) LOS and nLOS measurements. (b) Wall, closet and floor measurements.

Fig. 5. The floor plan of House3 with Tx and Rx locations for CW and SW measurements.

are partially carpeted. The heights of ceiling are all 2.4m. The internal walls have thickness of 12cm, and are made of gypsum board on wood studs separated by 41cm. The exterior wall is about 20cm thick with insulation materials inside and covered by plywood and plastic sidings. The thickness between floors is 33cm between basement and first floor, and 28cm between first and second floor. This house uses centralized heating and air conditioning systems with air supplied through metallic ducts located in the floors. Fig. 5 shows the floor layout and antenna locations for CW and SW measurements in House 3. Measurements for vertical polarization were carried out at all locations except locations indicated as lowercase 'b' in Fig. 5(b). For all measurements, Rx was placed in a corner of the family room as indicated by the star. Fig. 5(a) shows locations of Tx and Rx for LOS (denoted by 'A') and nLOS paths on the first floor for CW measurements. The nLOS paths include lightly blocked paths

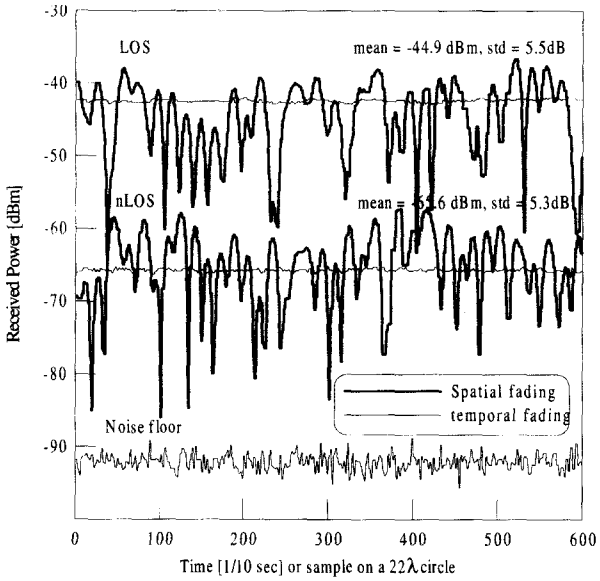

Fig. 6. Temporal and spatial fading at LOS and nLOS paths in Office1.

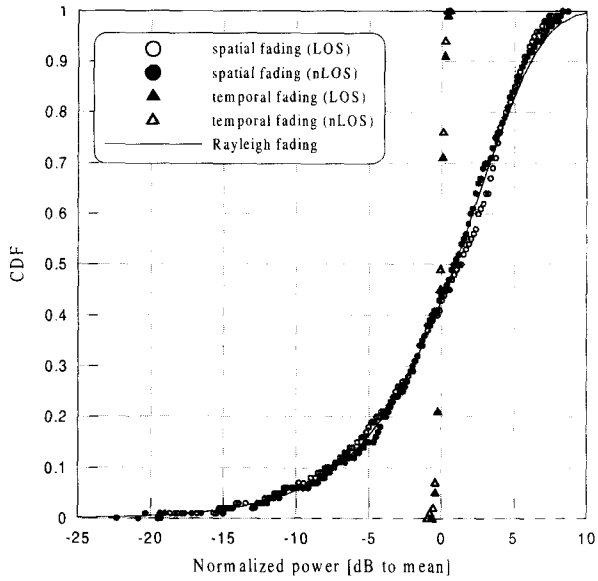

Fig. 7. Cumulative distributive function of the fadings shown in Fig. 6.

(denoted by 'B') and heavily blocked paths (denoted by 'C'). For a fixed distance between Tx and the axis of the Rx antenna rotator, the SW measurements were made at 24 equally spaced positions of Rx around the rotator circle. Fig. 5(b) shows the Tx and Rx locations for transmission loss measurements through the floors, walls, and a closet. For the measurement of floor transmission loss Rx was placed at the first and the second floor, while Tx was placed in the basement (denoted by 'b'). The wall and closet transmission loss were measured with Tx locations marked by 'W' with two corresponding Rx locations.

House 4 is a wooden-frame, three story single-family row house in Brooklyn, New York. It is over 100 years old and has frame constructions on the upper two floors. House 4 has a below-grade cellar and three different floor levels with wood floors that are fully carpeted. Measurements were made on the top two floors, whose ceiling heights are 3 m and 2.4m. The internal walls have thickness of 12cm, and are mostly of plaster on wood lath construction with wood studs separated by 41cm. The exterior walls are about 20cm thick with insulation materials inside and covered by wood and shingles. The thickness between floors is 22cm. House 4 uses steam heating with separate air conditioners for each room. The CW and SW measurements include LOS, nLOS, and between floor paths.

IV. CONTINUOUS WAVE (CW) MEASUREMENTS

A. Spatial and Temporal Fading Statistics

The observed signal at a receiver location is a summation of fields with different amplitudes and phases arriving from different directions because of scattering by furnishings and the building itself. The resulting summation exhibits rapid variation with position. To characterize the rapid local field variation, the received power is observed as the receiver is moved along the circle of circumference 22λ, while the transmitter is held stationary. Typical variations, measured using vertically polarized antennas in Office 1 are plotted in Fig. 6. These measurements were made under conditions when no one is moving in the vicinity of the radio link. Temporal fading for a fixed receiver position is also shown, and is seen to be very small. Temporal measurements at other receiver locations have different average levels given by the spatial fading pattern, but only very small time variation. The received power level for the moving receiver shows deep fading characteristics at both LOS and nLOS sites. Its average is called small area average.

Statistical analysis of the time or spatial variation of the received signal gives a probabilistic understanding of the indoor propagation channel. In general, it is known that spatial fading due to multipath for a site with a dominant LOS signal and several weak signals follows Ricean statistics, and when these weak signals approach the dominant signal level, the received signal variation approaches Rayleigh statistics. Cumulative distribution functions of the spatial and time fluctuations in Fig. 6 are shown in Fig. 7. Surprisingly, the measurement results show that the cumulative distribution function of spatial fading of the received signals measured by the rotating receiver follows the Rayleigh distribution no matter if the path conditions are LOS or nLOS. The Rayleigh distribution for LOS paths at 5.2GHz suggests that wall reflections and other scattering are stronger at this frequency, so that many of the arriving signals have more nearly equal amplitude. Because there was little movement in the physical environment during the measurements, the signal shows little variation with time. As a result, the cumulative distribution function of received signals measured as a function of time at a fixed receiver location exhibits a Ricean distribution no matter if the path conditions are LOS or nLOS. It is noted that similar results at 2.4 GHz were reported in [13].

B. Excess Path Loss

The excess path loss is obtained by subtracting the path loss in open area, as given by (2) and (3), from the small area average path loss. In Fig. 8(a), we have plotted the excess path loss in the office building using alphabet characters correspond-

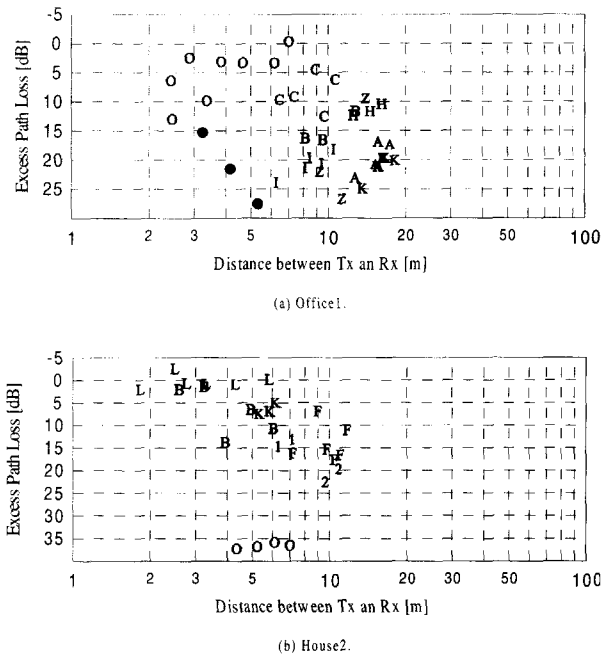

Fig. 8. Distribution of excess path loss on various radio links in Office1 and House2.

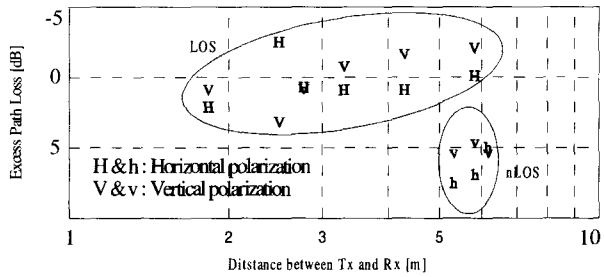

Fig. 9. Excess path loss for two polarizations on LOS and nLOS between floors in House1–4.

ing to the locations described in Fig. 2. At locations in room O, LOS paths have excess path loss of 0 to 13dB. Because this excess loss represents the small area average, it is not clear how the reflections and scattering effects make destructive contributions to the average on these LOS paths. Blockage by metallic workbenches and cabinets located to the right of the transmitter results in even greater excess path loss, as indicated by the filled O's for partially obscured paths. The path from the transmitter to locations in room A, K, and H go through 2 or 3 walls, and show a total excess path loss from 10 to 25dB. The direct measurement of transmission loss at gypsum board walls using directive horn antennas has found the loss to be 3–6 dB[14], [15]. Thus the excess path loss through 3 walls is expected to be 9–18dB. Allowing for metallic cabinets in the storage room, the nLOS path loss from room A, K, and H can be understood in terms of the wall transmission loss. Propagation to locations in room B, C, and I involves transmission through a single wall. The excess loss to locations in B and C are consistent with loss through sheetrock walls, when the metallic workbenches are allowed for. However, the excess loss to locations in I is significantly greater than expected.

In Fig. 8(b), the small area average received power and excess

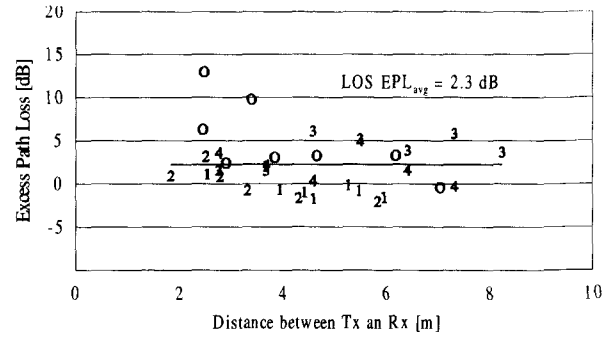

Fig. 10. Excess path loss for LOS links in Office1 and House1–4.

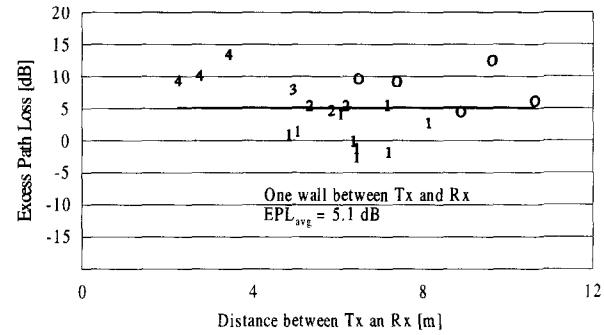

Fig. 11. Excess path loss for nLOS links with one wall blockage in Office1 and House1–4.

path loss are shown for receiver locations in and around House 2 indicated in Fig. 4. The LOS path indicated by 'L' in the living room has excess path loss between -2dB and 3dB centered at 0dB. The Rx locations in the kitchen 'K' are shadowed by one wall. The excess path loss at the 'K' locations is between 5dB and 7dB, which represents the penetration loss of internal walls. It is found that this estimation is consistent when the excess path losses in location '1' and '2' are compared. The major difference between '1' and '2' locations is the number of walls that the wave passes through. The path to locations '1' goes through a closet, while the path to location '2' goes through the closet and an additional wall. From the upper graph it is seen that the difference of excess path losses is also between 5dB and 7dB. The closet is composed of two internal walls and is completely filled with clothes and other items. Its penetration loss is between 14dB and 15dB. The excess path loss in the family room is between 7dB and 18dB depending on whether one or two walls block the path. The differences of excess path loss between groups can be understood in terms of the number of walls between Tx and Rx as previously described. The outdoor measurement at 'O' shows a significant attenuation of 36–37dB due to the metallic siding of the exterior wall. The excess path loss between floors ('B') shows wide variation of 2–14dB, which is to be compared with 7–10dB measured in House 1. It seems that metallic ducts between floors give this wide variation.

Fig. 9 shows a comparison of path losses for vertical polarization and horizontal polarization in House 2. Measurements were made in the living room (LOS) and the kitchen (nLOS) at the same Rx locations using the two polarizations. The result implies polarization does not affect the excess path loss of LOS

Table 1. Estimated wall and floor transmission loss [dB].

Building Element	Office 1	House 1	House 2	House 3	House 4	Average
Line of Sight	-1 ~ 13	-2 ~ 2	-2 ~ 3	2 ~ 6	-1 ~ 5	2.3
Interior One Wall	5 ~ 10	3 ~ 6	5 ~ 7	4 ~ 6	8 ~ 9	5.1
Interior Two Walls	21 ~ 23	4 ~ 5	–	9 ~ 13	15 ~ 18	13.7
exterior wall(sidings)	–	11~18(wooden)	36 ~ 37(metallic)	–	–	14.4/36.6
Closet	–	–	14 ~ 15	12 ~ 17	–	13.0
wooden floor(one floor)	–	7 ~ 10	2 ~ 14*	7 ~ 17*	5 ~ 10	8.9
wooden floor(two floors)	–	–	–	17 ~ 20*	–	18.6

*metallic duct grids between floors

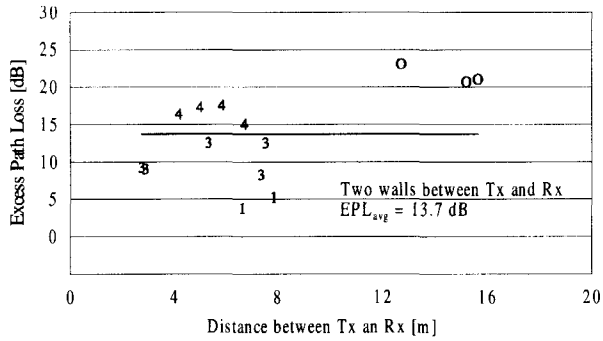

Fig. 12. Excess path loss for nLOS links with two wall blockage in Office1 and House1–4.

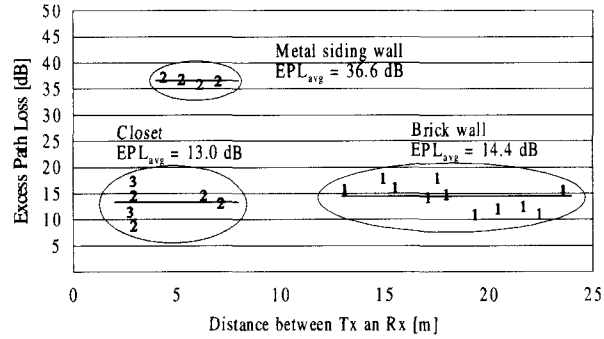

Fig. 13. Excess path loss for nLOS links with closet and exterior wall blockages in House1–4.

and nLOS paths.

Using the data gathered from all of the measurement sites, the excess path losses are shown in Fig. 10–14 for various type of blockage of the radio link. In these figures, the 'o' means the excess path loss measured at Office1, and the '1' through '4' correspond the excess path loss measured at House 1-4, respectively. The excess path loss is plotted as a function of distance in these figures to show that there is no systematic variation of excess path loss with distance. The mean values for each path type is indicated in the figures, and is listed in Table 1, along with the range of excess path loss observed in the different buildings. It is observed that the excess path loss can be understood in terms of the type and number of blockage elements, such as walls, closets, and floors between the transmitter and the receiver.

V. SWEPT FREQUENCY (SW) MEASUREMENT

The frequency response observed at three typical points around the rotator circle is shown in Fig. 15 for LOS and nLOS

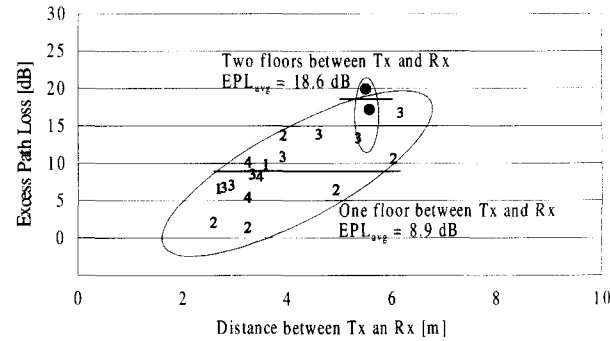

Fig. 14. Excess path loss for nLOS links between floors in House1–4.

paths in House 2. At any one point on the rotator circle, the received power is seen to fluctuate by 20 dB across the frequency band. It is noted that there is little difference between frequency responses for LOS and nLOS paths.

A. Coherence Bandwidth (CBW)

Let $Vi(f)$ be the voltage envelope at frequency f for a physical antenna position i. The envelope correlation coefficient $\rho(f, \Delta f)$ can be found by averaging over the antenna positions using the formula[16], [17]

$$\rho(f,\Delta f) = \frac{E[V_i(f)V_i(f+\Delta f)] - \bar{V}_i(f)\bar{V}_i(f+\Delta f)}{\sigma(f)\sigma(f+\Delta f)}. \quad (6)$$

The mean value is defined by

$$\bar{V}_i(f) = \frac{1}{N}\sum_{i=1}^{N} V_i(f), \quad (7)$$

and the standard deviation by

$$\sigma(f) = \sqrt{\frac{1}{N}\sum_{i=1}^{N}\left[V_i(f) - \bar{V}_i(f)\right]^2}. \quad (8)$$

The position index i refers to different locations around the rotator circle for one or more locations of the receiver cart, usually within the same room. Fig. 16 shows how the number of data sets used to find the CBW influences the stationarity of CBW over the frequency band from 5.15GHz to 5.35GHz in House 2. Fig. 16(a) shows the envelope correlation coefficient $\rho(f, \Delta f)$ found using 24 data sets at L1. In order to obtain more data sets, the SW frequency measurements were repeated in House 2 for receiver antenna at the locations of L and K, indicated in

Table 2. Δf variation at $\rho(f,\Delta f) = 0.5$ over the frequency range in Fig. 16.

	location	distance	number of data sets	Coherence Bandwitdth [MHz]			
				mean	min	max	std
original	L1	5.6 m	24	15.7	3.5	38.8	7.7
repeated	L1	5.6 m	120	17.2	7.7	24.5	4.7
	L2	3.5 m	96	9.4	5.0	14.9	2.0
	L3	6.6 m	24	18.3	6.4	38.9	7.6
	K1	4.5 m	24	11.6	4.1	36.6	8.1
	overall	–	240	13.3	7.3	20.5	2.8

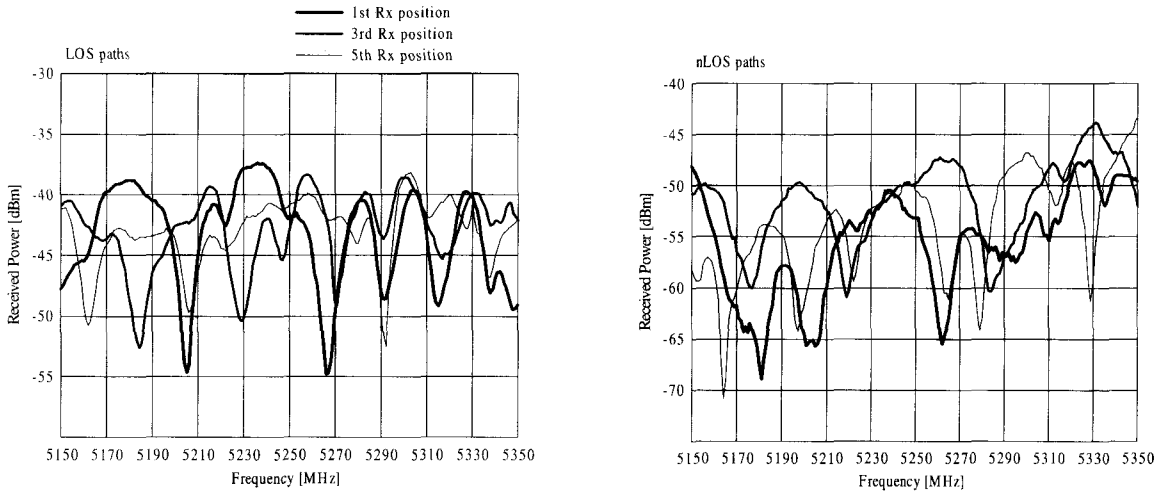

(a) LOS paths sets. (b) nLOS paths sets.

Fig. 15. Typical swept frequency responses on LOS and nLOS links in House2 when Rx is positioned at three different points on the rotator circle.

Table 3. Overall CBW and RMS delay spread (τ_{rms}) from 5.15GHz to 5.35GHz.

Tx-Rx	site	Area [m^2]	data sets	CBW [MHz]	τ_{rms} [nsec]
LOS	Office 1	75	48	4.4	38.1
	House 1	35	32	12.2	14.8
	House 2	34	240	13.3	12.1
	House 3	46	120	7.9	20.6
	House 4	30	120	11.7	14.8
nLOS	Office 1	–	48	2.7	62.3
	House 1	–	30	11.0	15.8
	House 2	–	48	12.5	13.0
	House 3	–	58	7.4	21.7
	House 4	–	44	12.0	14.2
Between floors	House 1	–	12	16.6	11.8
	House 2	–	24	17.0	9.2
	House 3	–	46	17.6	9.5

Fig. 4(b). In Fig. 16(b), we have plotted $\rho(f, \Delta f)$ obtained when 240 data sets are used corresponding to a second set of measurements at L1, and measurements at L2, L3, and K1. The number of measurement points at each location is summarized in Table 2 for the various measurements. It is seen that the 240 locations used to construct Fig. 16(b) gives a smoother, less wrinkled 3-dimensional graph than do the 24 locations in Fig. 16(a).

The coherence bandwidth (CBW) for each frequency f is defined as the value of Δf such that $\rho(f, \Delta f) = 0.5$. The mean value of CBW for all frequencies, its minimum and maximum values, and its standard deviation are listed in Table 2 for the different number of data sets used to find $\rho(f, \Delta f) = 0.5$. The values in Table 2 imply that averaging over more data sets decreases the variation range of Δf and its standard deviation without significantly changing the mean value (15.7MHz vs 13.3MHz). The foregoing procedure is used in the following section to obtain CBW of the wireless channel in various indoor environments from the envelope correlation coefficient of (6).

The mean values of CBW obtained on various radio paths in the different buildings are summarized in Table 3. Typical results of the CBW for Office 1, House 1 and House 2, are plotted in Fig. 17, showing the variation with frequency in the range from 5.15GHz to 5.35GHz. The LOS path includes averaging over all data sets measured in the same room, and the nLOS path includes paths with one wall and two wall blockages. It is noted that the overall average CBW's in the houses are very close to 7–14MHz for both LOS and nLOS paths, while the average is 3–5MHz in Office 1. The lower value of CBW in Office 1, resulting in a longer delay spread, may be due to the fact that the rooms of Office 1 are larger than those of the houses. The discrete peaks that can be seen in nLOS paths of Fig. 17, seem to be from the small number of measure data sets. The average CBW in paths between floors was observed to be 16–18 MHz.

B. RMS Delay Spread

As a mathematical model of indoor wireless channel, we use Jakes' approach [16], in which statistical properties are computed on the basis of ensemble averages in the wide sense stationary uncorrelated scattering (WSSUS) channel. If the power delay profile is assumed to have the exponentially decaying time

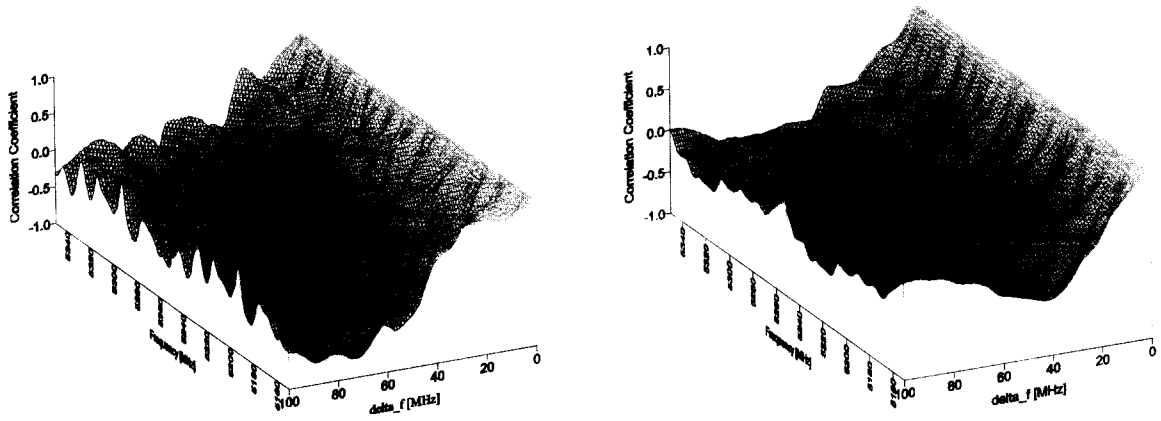

(a) Surface plot using 24 data. (b) Surface plot using 240 data.

Fig. 16. Surface plot of envelope correlation coefficients using different number of data sets.

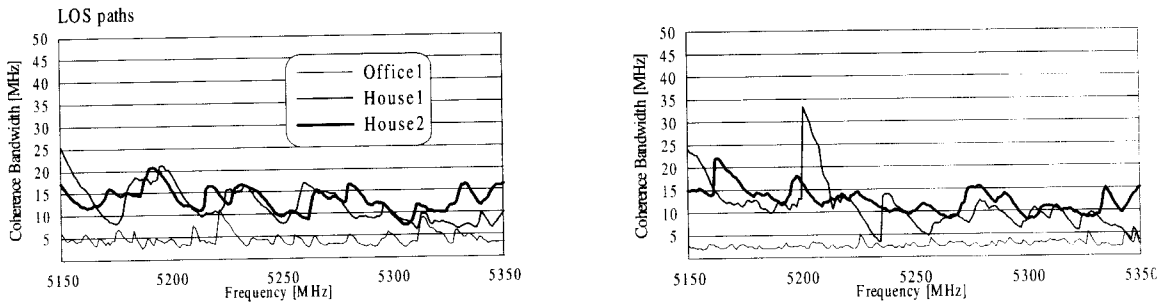

(a) LOS paths. (b) nLOS paths.

Fig. 17. Coherence bandwidth as a function of frequency in Office1 and House1-2.

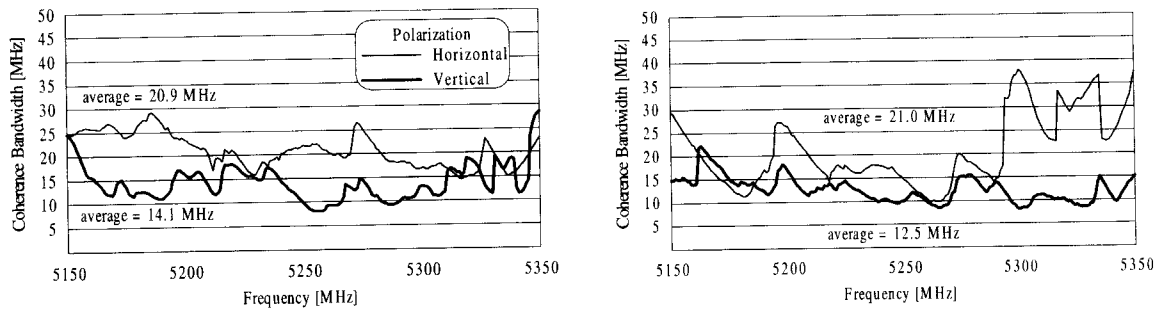

(a) LOS paths. (b) nLOS paths.

Fig. 18. Coherence bandwidth as a function of frequency for different polarizations in House2.

dependence of the form [9]

$$p(\alpha, T) = \frac{1}{2\pi\tau_{rms}} e^{-T/\tau_{rms}}, \tag{9}$$

where τ_{rms} is the RMS delay spread, the coherence bandwidth is given by

$$\tau_{rms} = \frac{1}{2\pi CBW}. \tag{10}$$

Using the equation (10), the mean RMS delay spread was calculated as shown in Table 3. It is seen that the mean RMS delay in the houses has a range of 12–22nsec for both LOS and nLOS paths, and of 16–18nsec for paths between floors. In the office building, the mean RMS delay spread was found to be 38 nsec and 62nsec for LOS and nLOS paths, respectively. As is to be expected, the larger rooms in the office building give larger delay spread than that is found in the houses.

C. Polarization Effects

To examine the polarization effects on the CBW in a room SW measurements with vertical and horizontal polarized anten-

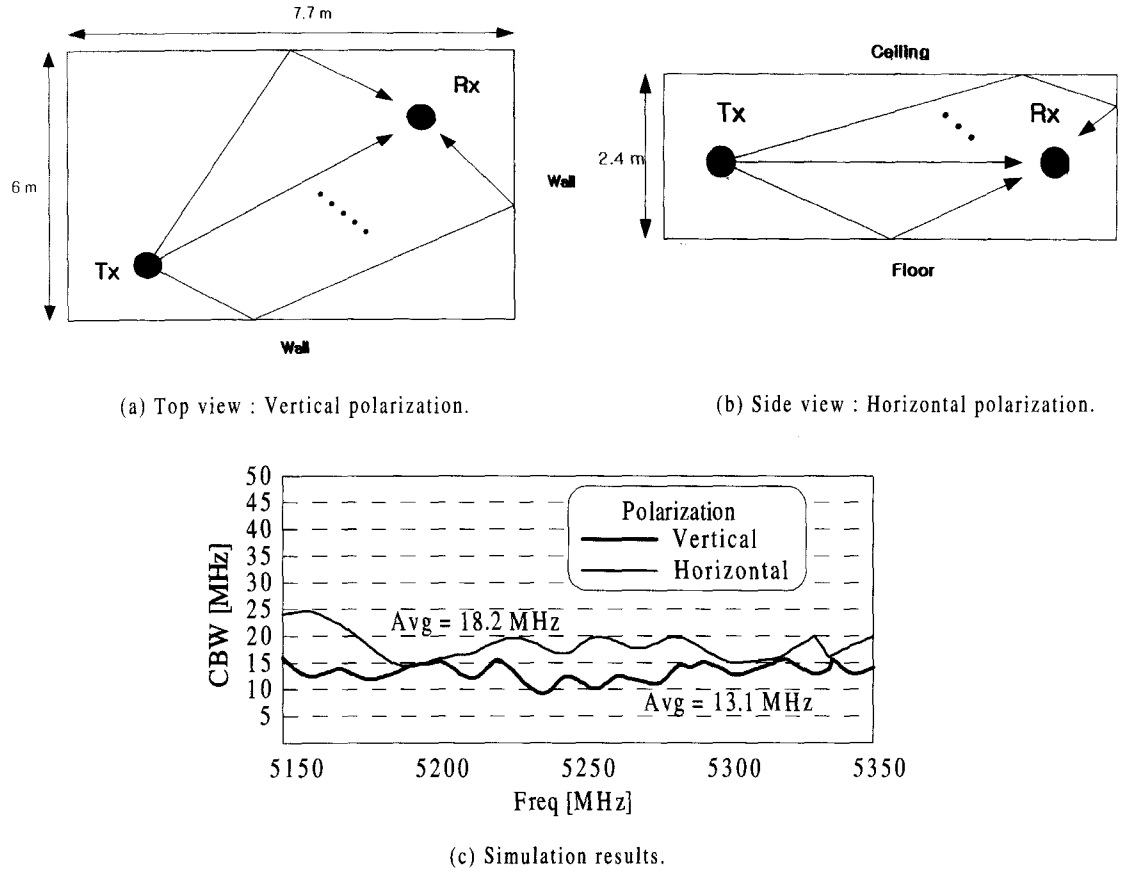

(a) Top view : Vertical polarization.

(b) Side view : Horizontal polarization.

(c) Simulation results.

Fig. 19. Simulation results of coherence bandwidth for different polarizations on LOS paths in an idealized rectangular room.

nas were performed at LOS and nLOS paths at the locations of House2, shown in Fig. 4(b). The results are plotted in Fig. 18. It is found that the horizontal polarization has a CBW that is 7–8MHz larger than the vertical polarization for LOS and nLOS paths.

Considering 9 dBi gain and 14° beamwidth of the colinear antennas used for the measurements, major contributions to the received power seems to be from the wall reflections in case of vertical polarization, while it is from floor and ceiling reflections in case of horizontal polarization. This polarization effect was modeled as shown in Fig. 19(a) and (b). We assume a vacant rectangular room without furniture having dimensions equal to that of the living room in House 2. There are four different Rx locations having LOS paths in Fig. 4(b), and each location has 24 different positions along the rotator circle. The received power Prx is simulated by summing all possible rays that undergo up to two reflections. The relative dielectric constant of walls ε_γ is assumed to be 4.4 and the simulation considers only reflections by walls or ceiling/floor for each polarization. The simulations were repeated for four different Rx locations. Finally the simulation data for all Rx locations was used to calculate CBW of LOS paths in the rectangular room. The simulation results shown in Fig. 19(c) indicate that the CBW for horizontal polarization is 5.1 MHz larger than for vertical polarization. This difference explains the measured CBW results for the two polarizations shown in Fig. 18. A similar result was reported at 94GHz [18].

D. Effect of Distance and Room Area on Delay Spread

To obtain the dependence of RMS delay spread on room area for LOS paths, SW measurements were repeated in classrooms and auditoriums having different room areas in two school buildings (Office1 and Office2). Previous measurements [4]–[6], [8], and [18], [19] indicate that the room size and the separation between transmitter and receiver have a large effect on the time dispersive characteristics of indoor channels. The mean RMS delay spread is plotted as a function of room area in Fig. 20(a), which shows that the delay spread increases as room area increases. The dependence of mean RMS delay spread on the separation between transmitter and receiver at LOS paths in the same room is plotted in Fig. 20(b). It is seen that the delay spread decreases with increasing separation.

VI. CONCLUSION

Measurements indicate that in most cases the average path loss at 5.2GHz can be characterized as the sum of the free space loss and wall or floor penetration loss, whose values are suggested in Table 1. These values are not dependent on the polarization. However furniture can cause significant blockage even for paths in the same room, and furniture against walls can add to the wall loss, as demonstrated in the office building.

The fading statistics measured with a rotating receiver shows that cumulative distribution function of the received signal at 5.2GHz inside buildings follows the Rayleigh distribution no

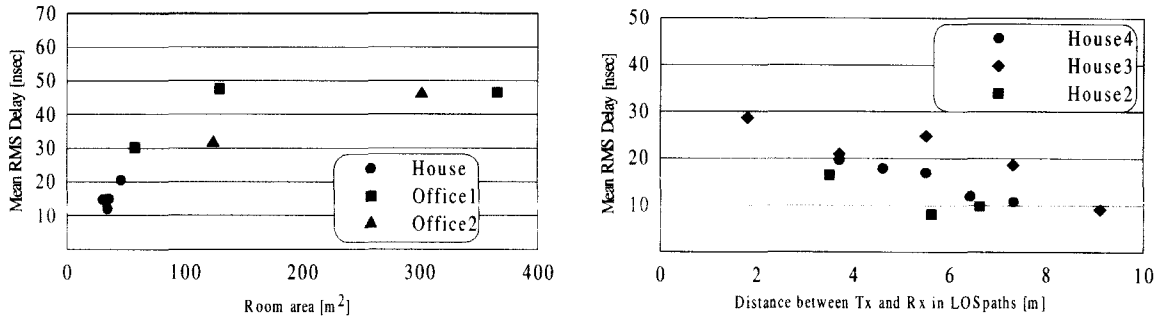

Fig. 20. Dependence of RMS delay spread on room area and Tx-Rx separation at LOS paths.

matter if the path conditions are LOS or nLOS.

Based on measurements of the swept frequency response from 5.15GHz to 5.35GHz in an office building and four houses, the coherence bandwidth (CBW) and RMS delay spread were calculated and are suggested in Table 3. It is found that CBW is sensitive to Rx locations even when they are within the same room. The overall mean CBW in the houses is 7–14MHz for both LOS and nLOS paths. In Office 1, CBW is 3–5MHz which is lower than in the houses. This implies that an office building with its larger rooms has longer delay spread than the houses. The measurements show that the horizontal polarization gives larger CBW than the vertical polarization by 7–8MHz for LOS and nLOS paths. This agrees well with the simulation result for LOS paths. If less directive antennas are used, the CBW for both polarizations should be more nearly equal to that measured for vertical polarization. In houses the mean RMS delay spread has a range of 12–22nsec for LOS and nLOS paths, and 9–12nsec for paths between floors. It is also found that RMS delay spread increases with room area, as in the office building, and decreases with distance between transmitter and receiver when they are in the same room.

REFERENCES

[1] R. V. Nee and G. Awater, "New high-rate wireless LAN standards," *IEEE Commun. Mag.*, Dec. 1999.

[2] R. O. LaMaire, A. Krishna, and P. Bhagwat, "Wireless LANs and mobile networking: Standards and future directions," *IEEE Commun. Mag.*, Aug. 1996.

[3] A. Affandi, G. E. Zein, and J. Citerne, "Investigation on frequency dependence of indoor radio propagation parameters," in *Proc. IEEE Veh. Techol. Conf.*, Dallas, TX, 1999, pp. 1988–1992.

[4] G. J. M. Janssen, P. A. Stigter, and R. Prashad, "Wideband indoor channel measurements and BER analysis of frequency selective multipath channels at 2.4, 4.75, and 11.5 GHz," *IEEE Trans. Commun.*, vol. 44, no. 10, pp. 1272–1288, Oct. 1996.

[5] C. Bergljung and P. Karlsson, "Propagation characteristics for indoor broadband radio access networks in the 5 GHz band," *IEEE Int. Symp. Personal, Indoor and Mobile Radio Commun.*, vol. 2, 1998, pp. 612–616.

[6] P. Nobles and F. Halsall, "Delay spread measurements within a building at 2 GHz, 5 GHz, and 7 GHz," *IEE Colloquium Propagation Aspects of Future Mobile Systems*, pp. 8/1–8/6, 1996.

[7] P. Nobles, D. Ashworth and F. Halsall, "Indoor radiowave propagation measurements at frequencies up to 20 GHz," in *Proc. IEEE Veh. Techol. Conf.*, Sweden, 1994, pp. 873–877.

[8] P. Hafezi *et al.*, "Propagation measurements at 5.2 GHz in comercial and domestic environments," *IEEE Int. Symp. Personal, Indoor and Mobile Radio Commun.*, vol. 2, 1997, pp. 509–513 .

[9] S. Guerin, Y. J. Guo, and S. K. Barton, "Indoor propagation measurements at 5 GHz for HIPERLAN", in *Proc. IEEE Int. Conf. Antenna and Propagation*, vol. 2, 1997, pp 306–310.

[10] I. Cuinas, M. S. Varela, and M. G. Sanchez, "Wide band indoor radio channel measurements at 5.8 GHz," in *Proc. IEEE Veh. Tech. Conf.*, Boston, 2000.

[11] H. L. Bertoni, *Radio Propagation for Modern Wireless Systems*, Prentice Hall, 2000.

[12] W. Honcharenko, H. L. Bertoni, and J. L. Dailing, "Bilateral averaging over receiving and transmitting areas for accurate measurements of sector average signal strength inside buildings," *IEEE Trans. Antennas Propagation*, vol. 43, pp 508–512, 1995.

[13] S. C. Kim and H. L. Bertoni, *Modeling and Analysis of Indoor Wireless Communication Channel*, Ph.D dissertation, Polytechnic Univ., July 1995.

[14] H. K. Chung and H. L. Bertoni, *Indoor Propagation Characteristics at 5.2GHz : Continuous Wave & Swept Frequency Measurements in an Office Building and Residential Houses*, Final report to Sharp Lab. of Americal Inc., Polytechnic Univ., 2000.

[15] G. Durgin, T. S. Rappaport, and H. Xu, "Measurements and models for radio path loss and penetration loss in and around homes and trees at 5.85 GHz," *IEEE Trans. Commun.*, vol. 46, no, 11, pp. 1484–1496, Nov. 1998.

[16] W. C. Jakes, *Microwave Mobile Communications*, IEEE Press, 1974.

[17] M. D. Yacoub, *Foundation of Mobile Radio Engineering*, CRC Press, 1993.

[18] A. Kajiwara, "Effects of polarization, antenna directivity, and room size on delay spread in LOS indoor radio channel," *IEEE Trans. Veh. Technol.*, vol. 46, pp. 169–175, Feb. 1997.

[19] R. J. C. Bultitude *et al.*, "The dependence of indoor radio channel multipath characteristics on transmitter/receiver ranges," *IEEE J. Select. Areas Commun.*, vol. 11, pp. 979–990, Sept. 1993.

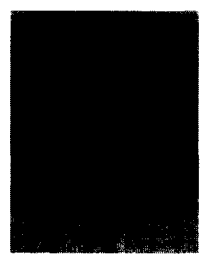

Hyun Kyu Chung received the B.S. degree in electrical engineering from Seoul National University, Seoul, Korea, in 1985 and the M.S. and Ph.D. degrees in electrical engineering from Korea Advanced Institute Science and Technology (KAIST), Seoul, Korea, and Polytechnic University, Brooklyn, New York, in 1988 and 2000, respectively. From 1988 to 1993, he worked with Korea Telecom as a Research Engineer, where he developed AT&T no. 1A ESS translation data administration system (NODAS) and participated in SS7 testing and the IN service design. From 1994 to 1998, he worked with SK Telecom where he was a technical staff in the CDMA task force team and project manager in SK telecom U.S. Research and Development Center. After working in Wireless Network Group of Lucent Technologies as a member of technical staff for WCDMA system engineering, he joined Electronics and Telecommunications Research Institute (ETRI) in 2001. His research interests include radio propagation, diffraction theory, spread spectrum communication, and spatial channel modeling for MIMO systems.

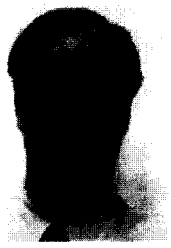

Henry L. Bertoni received the B.S. degree in Electrical Engineering from Northwestern University, Evanston, IL. in 1960, as well as the M.S. degree in Electrical Engineering in 1962, and the Ph.D. degree in Electrophysics in 1967, both from the Polytechnic Institute of Brooklyn (now Polytechnic University) After graduation he joined the faculty of the Polytechnic, eventually becoming Head of the EE Department (1990–95), and serving as Vice Provost of Graduate Studies (1995–96). His research has dealt with theoretical aspects of wave phenomena in electromagnetics, ultrasonics, acoustics and optics. He has authored or co-authored over 70 journal papers on these topics, of which three have received best paper awards. During 1982–83 he spent sabbatical leave at University College London as a Guest Research Fellow of the Royal Society. His current research electromagnetics deals with the theoretical prediction of UHF propagation characteristics in urban environments. He and his students were the first to explain the mechanisms underlying characteristics observed for propagation of the Cellular Mobile Radio signals. Much of this work is described in his recent book Radio Propagation for Modern Wireless Systems, Prentice Hall PTR, 2000. Dr. Bertoni is a Fellow of the IEEE. He was the first Chairman of the Technical Committee on Personal Communications of the IEEE Communications Society, and was IEEE representative to, and chairman of the Hoover Medal Board of Award. He has served on the ADCOM of the IEEE Ultrasonics, Ferroelectric and Frequency Control Society, and is also a member of the International Scientific Radio Union and the New York Academy of Science. He has just finished a two year appointment as Distinguished Lecturer of the IEEE Antennas and Propagation Society.